https://dx.doi.org/10.1016/j.atmosenv.2020.117550

Long-term temporal variations and source changes of halocarbons in the Greater Pearl River Delta region, China

Lewei Zeng[1#], Juan Dang[1#], Hai Guo[1*], Xiaopu Lyu[1], Isobel J. Simpson[2], Simone Meinardi[2], Yu Wang[1], Luyao Zhang[1], Donald R. Blake[2]

[1]Air Quality Studies, Department of Civil and Environmental Engineering, The Hong Kong Polytechnic University, Hong Kong, China

[2]Department of Chemistry, University of California at Irvine, USA

*Corresponding author. ceguohai@polyu.edu.hk

[#] These authors contributed equally to this work.

Highlights:

1. Mixing ratios of CFCs (CFC-11, CFC-12 and CFC-113) decreased over the past 18 years except for CFC-114, which increased in the Greater PRD region.
2. Refrigeration applications were the main sources of halocarbons in the Greater PRD region.
3. Refrigeration industry dominated by CFCs decreased during the past 18 years, while source of CFCs replacement increased.
4. Based on the measured ratios of halocarbons to CO, the estimated total halocarbon emissions in 2016 were 46.5 ± 16.7 Gg for the whole Greater PRD region.

Abstract

Halocarbons are widely used in the Greater Pearl River Delta (PRD) region of China. To study the long-term trends, source changes and emissions of major halocarbons, a total of 1505 canister air samples were collected in the Greater PRD region during 2001-2018. Mixing ratios of CFCs decreased significantly over the past 18 years except for CFC-114, which significantly increased in the Greater PRD, consistent with the recent observations of significant CFC-114 emissions in East Asia. Declines in CFCs in the Greater PRD region were faster than those at the background Mauna Loa (MLO) site, indicating effective control regulations. Source apportionment simulations showed that refrigeration applications, including refrigeration industry and CFCs replacement, were the main sources of halocarbons. During the study period, refrigeration industry experienced a progressive decline in both mixing ratio and percentage, while the contribution of CFCs replacement remained increasing. Contribution of solvent use in electronic industry traced by C_2Cl_4 dramatically decreased during the study period, and stayed at a low level in recent years. Based on the measured ratios of halocarbons to CO, the estimated total halocarbon emissions in 2016 were 46.5 ± 16.7 Gg for the Greater PRD region. This study provides useful information for examining the evolving emission status of halocarbons in the Greater PRD region in response to control strategies and changing usage.

Keywords: Halocarbons; Long-term trends; Greater Pearl River Delta; Source apportionment; Emission estimation

1. Introduction

Halocarbons are an important category of volatile organic compounds (VOCs), and are extensively used as foam blowing agents, refrigerants, aerosol propellants, dry cleaning solvents, degreasing agents, feedstock for chemical production, and fire extinguishing agents [*Godish*, 2003]. Among the halocarbons, chlorofluorocarbons (CFCs) and hydrochlorofluorocarbons (HCFCs) are ozone-depleting substances (ODSs) due to their long atmospheric lifetimes and catalytic impact on ozone decomposition in the stratosphere. Hydrofluorocarbons (HFCs) were then introduced as replacements of HCFCs and CFCs because of their near-zero ozone depletion potential (ODP) values [*Fortems-Cheiney et al.*, 2013; *Hundy et al.*, 2016]. However, because HFCs are powerful greenhouse gases, their emissions may make an increasing contribution to global radiative forcing [*Ou-Yang et al.*, 2015; *Simmonds et al.*, 2017; *Velders et al.*, 2015]. Given their high ODP, production and emissions of many halocarbons have been regulated under the Montreal Protocol and its amendments [*Grubb et al.*, 1999; *Maione et al.*, 2011].

Mainland China belongs to the "Article 5" in the Montreal Protocol. According to the reduction plans, the production and consumption (usage) of CFCs was banned in mid-2007 with the exception of the exempted uses [*WMO/UNEP*, 2018]. The consumption of HCFCs was frozen in 2013 at the baseline of the average 2009-2010 level, with a goal of 10% reduction by 2015 and 35% by 2020. For Hong Kong (HK), as a "non-Article 5" party, the consumption of CFCs was phased out in 1996, and with a goal of 90% reduction of HCFC consumption by 2015 and 100% by 2030 [*Fang et al.*, 2012; *HKEPD*, 2018*a*; *Hurst et al.*, 2006]. As global production and consumption of CFCs was phased out in response to the Montreal Protocol, the leakage of CFCs in existing products and landfills, referred as "banks", could become the important sources of CFCs emission in the future [*Zhang et al.*, 2010a]. However, it is important to note that some ODSs (e.g. CFC-11) are not decreasing in the atmosphere as quickly as expected based on the Montreal Protocol, implying ongoing emissions that appear to be unreported new production rather than release from banks [*Rigby et al.*, 2019; *SPARC*, 2017; *Lunt et al.*, 2018; *Montzka et al.*, 2018]. As temporary substitutes of CFCs and HCFCs, the consumption and production of HFCs are increasing steeply in developing countries since CFCs were banned and the consumption of HCFCs was frozen [*Su et al.*, 2015].

Besides CFCs and their replacements, other halocarbons also play important roles in ozone depletion processes in the stratosphere. CH_3CCl_3 is of particular interest since its atmospheric mass budget has been used to estimate ambient concentrations of the hydroxyl radical (OH) [*Prinn et al*,. 1987; *Gentner et al.*, 2010]. CCl_4 was used as a feedstock in the production of CFC-11 and CFC-12, and it is still used as a feedstock in certain countries [*Hurst et al.*, 2004; *Harrison et al.*, 2017; *WMO/UNEP*, 2018]. According to the terms of the Montreal Protocol and its Amendments, production and consumption of CH_3CCl_3 and CCl_4 were both banned in developed countries in 1996 and in developing countries in 2015 and 2010, respectively [*Hurst et al.*, 2006; *Harrison et al.*, 2017; *WMO/UNEP*, 2018]. Bromine also plays an important role in stratospheric ozone destruction. Halons, with solely anthropogenic sources, were primarily used as fire suppressants [*Fraser et al.*, 1999]. H-1211, H-1301 and H-2402 are major halons in the troposphere, which have been phased out in HK by 1994, and in mainland China by 2007. CH_3Br, another type of bromine, is released from both natural sources (oceans, biomass burning, rice paddies and other terrestrial ecosystems) and anthropogenic sources (soil fumigation and leaded gasoline) [*Yokouchi et al.*, 2002; *Maione et al.*, 2011], and its anthropogenic uses have been prohibited under the Montreal Protocol, except some consumption in quarantine and pre-shipment applications [*WMO/UNEP*, 2018; *Yvon-Lewis et al.*, 2009]. CH_3Cl, the most abundant halocarbon, is mainly emitted from biomass burning, oceans, tropical vegetation, coal combustion and waste incineration [*Blake et al.*, 1996; *Li et al.*, 2017; *Maione et al.*, 2011; *Wang et al.*, 2005; *WMO/UNEP*, 2018; *Youkouchi et al.*, 2000]. CH_3Cl is also commonly used as a solvent, processing agent and feedstock for chemical production in China [*Li et al.*, 2017], and *Guo et al.* [2009] speculated that about 40% of the CH_3Cl in the Greater Pearl River Delta (PRD) of China was emitted from solvent usage in the production processes of refrigerants. C_2Cl_4 is primarily used as a dry cleaning solvent and degreasing agent, and its predominant anthropogenic source makes it an excellent marker for industrial pollution [*Simpson et al.*, 2004].

Furthermore, some very short lived substances (VSLS), such as CH_2Br_2, $CHBr_3$ and CH_3I, are largely produced by oceanic emissions [*Lennartz et al.*, 2015]. CH_2Cl_2, another VSLS, with an emission distinctly increased in the troposphere in the past decade [*Oram et al.*, 2017]. It is widely used as solvents in paints, paint strippers and degreasing processes, and as an aerosol propellant and a blowing and cleaning agent in foam production [*Borkar et al.*, 2010]. Besides, CH_2Cl_2 was recently reported to be used as a feedstock in the production of HFC-32 [*Leedham Elvidge et al.*, 2015], which is the main ingredient of the refrigerant R-410A increasingly used in new indoor air-conditioning to replace HCFC-22 [*Fang et al.*, 2016]. Although VSLS are not regulated by the Montreal Protocol due to their short atmospheric lifetimes and low ODPs, a recent study indicated their growing threat to the O_3 layer [*Oram et al.*, 2017].

The inner PRD region is located in Guangdong province in southern China, and consists of nine cities (Guangzhou, Shenzhen, Zhuhai, Dongguan, Zhongshan, Foshan, Jiangmen, Huizhou, and Zhaoqing), while the Greater PRD region extends the inner PRD region to Hong Kong and Macau (Figure 1). As a heavily populated and leading manufacturing region, the atmospheric abundances and trends of halocarbons in this region have attracted much attention and been the focus of several measurement studies in the past two decades. *Chan and Chu* [2007] analyzed halocarbons in the inner PRD region in 2000, while halocarbons were analyzed in 45 Chinese cities including the PRD region in winter 2001 [*Barletta et al.*, 2006]. *Guo et al.* [2009] analyzed halocarbons from 2001 to 2002 and investigated their source origins in both inner PRD and HK. *Shao et al.* [2011] reported the mixing ratios of halocarbons in 2004 in the PRD region and estimated their emissions, and *Zhang et al.* [2014] investigated the spatial variations of CFCs and HCFC-22 in 2008 and 2009 in the PRD region. However, there are limited studies on the long-term variations of halocarbons as well as their source changes since the 2010 phase-out in China [*Su et al., 2015*]. *Zhang et al.* [2010b]

studied long-term variations and emission patterns of halocarbons from 1998 to 2008 in the Greater PRD region. Therefore, more updated studies are needed to examine the temporal variations and emission status of halocarbons in the Greater PRD region.

In this study, comprehensive field measurements were carried out from 2001 to 2018 at different sites in the Greater PRD region. The data provide an opportunity to investigate the long-term variations, source changes and emissions for halocarbons, and infer the implementation status of the Montreal Protocol in the Greater PRD region.

2. Methodology

2.1 Description of the Sampling Sites

In this study, the inner PRD sampling sites were Dinghu, Qingyuan, Wanqingsha, Wanshan Island, Qi'ao Island, and Conghua. In addition, field campaigns were carried out in HK at Hok Tsui, Tai O, Tung Chung and Tai Mo Shan (Figure 1). Some of the sampling sites were ambient air quality monitoring stations established by the local governments while others were set up by our group. Detailed information of the sampling sites and corresponding sampling time are presented in Table 1. Briefly, the Dinghu site, located in Zhaoqing, was a rural site surrounded by tropical forest [*Chan et al.*, 2006a]. Qingyuan site was a rural area in northwestern Guangzhou [*Zhang et al.*, 2008]. Wanqingsha, surrounded by croplands and some clothing workshops, was a suburban site in southern Guangzhou [*Zhang et al.*, 2010b]. In addition, there was another rural site (Conghua) in the northeastern Guangzhou surrounded by lakes and forests. The remote Wanshan Island site was in the South China Sea and the distance from this island to urban centers of Hong Kong, Macau and Zhuhai was about 64 km, 35 km and 40 km, respectively [*Wang et al.*, 2018]. The rural Qi'ao Island site was located in the northeastern Zhuhai, on the west bank of the Pearl River Estuary. Hok Tsui was a background site situated at the south tip of HK with sparse anthropogenic sources [*Lee et al.*, 2002]. Tai O, a rural/coastal site in southwestern HK, was about 32 km from the urban center [*Wang et al.*, 2005]. Tung Chung was situated on northern Lantau Island and was a typical suburban site receiving both local and regional air masses. Tai Mo Shan site was located in the summit of the highest mountain in HK, surrounded by Country Parks to the east, south, and west, and defined as a suburban site [*Ling et al.*, 2014]. On the whole, the air samples collected at these sites were representative of typical local halocarbon levels in the atmosphere since all the sampling sites were suburban and/or rural locations with similar geographical proximity, distant from emission sources.

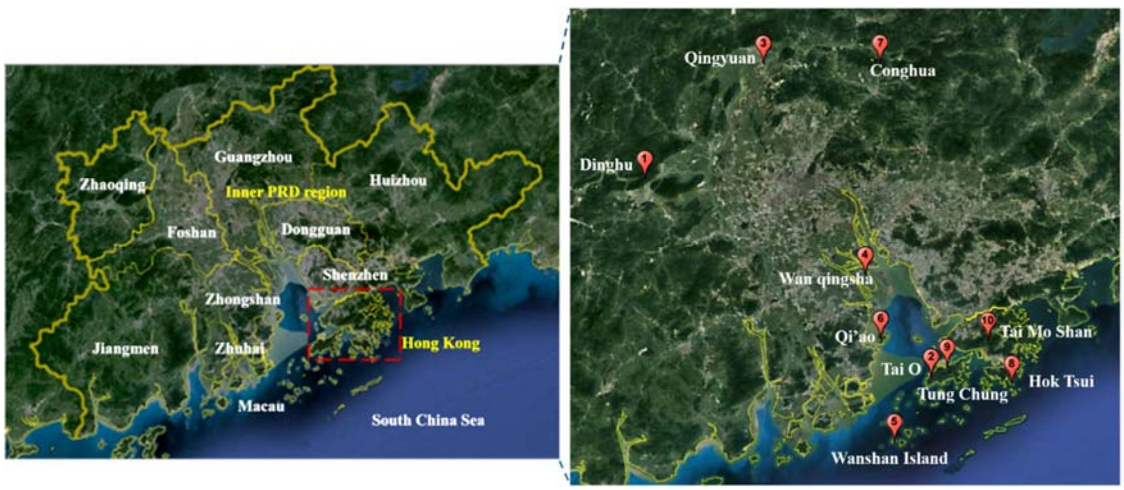

Figure 1. Locations of the Sampling Sites in the Greater Pearl River Delta Region

Table 1. Description of the Sampling Sites for the Field Campaigns

Site	City	Longitude (°)	Latitude (°)	Site Type	Sampling Time	Number of samples
Dinghu	Zhaoqing	112.56	23.15	Rural	3/3/2001-3/19/2001	39
Qingyuan	Qingyuan	113.05	23.69	Rural	2/29/2004-4/13/2004	33
Wanqingsha	Guangzhou	113.55	22.71	Rural	4/20/2004-6/29/2004; 10/26/2007-12/1/2007	88 102
Wanshan Island	Zhuhai	113.70	21.93	Marine Background	9/11/2013- 11/21/2013	170
Qi'ao	Zhuhai	113.65	22.42	Rural	10/14/2016-11/18/2016	118
Conghua	Guangzhou	113.62	23.65	Rural	1/18/2018- 1/23/2018; 6/29/2018-7/4-2018	36
Hok Tsui	Hong Kong	114.25	22.21	Rural	3/3/2001-4/22/2002	79
Tai O	Hong Kong	113.85	22.26	Rural	5/3/2002-12/31/2002	109
Tai O (Regional)[a]	Hong Kong	113.85	22.26	Rural	10/10/2001-3/6/2002	28
Tung Chung	Hong Kong	113.96	22.29	Suburban	1/6/2003-8/28/2003; 9/12/2006-2/22/2008; 9/11/2013-11/21/2013; 11/1/2016-11/18/2016	40 155 148 187
Tai Mo Shan	Hong Kong	114.12	22.40	Rural	9/28/2010-11/21/2010	201

a. Regional air masses from inner PRD region obtained by backward Lagrangian particle release simulations [*Guo et al.*, 2009].

2.2 Sampling and Chemical Analysis

Whole air samples were collected in 2-L stainless steel canisters with electro-polished inner surface, which were conditioned beforehand. Prior to sampling, canisters were repeatedly cleaned at least four times by filling and evacuating zero air. Then, all cleaned canisters were evacuated to 180 mtorr for sampling. A total of 1505 ambient air samples were collected on selected days from 2001-2018, and sometimes multiple samples were collected in one day. The sampling flow rate was ~35 mL/min and sampling duration was one hour. After collection, samples were shipped to the laboratory for chemical analysis within two weeks. 250 mL of each sample were transferred to a pre-concentrator, concentrated with liquid nitrogen, and injected into a gas chromatography-mass selective detector / electron capture detector (GC-MSD / ECD) system. Most target substances were analyzed using ECD, while HCFCs, HFCs, CFC-113, H-1211, CH_3Cl, CH_2Cl_2 and CH_3Br were measured using MSD in selected ion monitoring (SIM) mode (target ions are listed in Table S1). Calibration standards were produced and regularly quantified by the Rowland/Blake laboratory in the University of California at Irvine (UCI). They followed the same protocols to prepare their own standards for decades in order to keep consistency across standards maintained and during the course of this study. Calibration curves were made with at least five points ranging from 0 to 4 ppbv for quantification of the target halocarbons. Linear correlation coefficients (R^2) between the responses and standard concentrations were all above 0.995. Accuracy, replicate precision and method detection limit for each species were calculated according to TO-14A/15 methods issued by USEPA (see detailed description in Text S1), which were 1.3 to 8.0 %, 0.2 to 7.9 % and 0.2 to 5.7 pptv, respectively (Table S1).

Samples collected in earlier years (prior to 2013) were analyzed in the UCI laboratory, while more recent samples were mainly measured in our laboratory at the Hong Kong Polytechnic University (HKPU) using the same analytical method as that in the UCI laboratory (the analytical systems in our laboratory were established following the prototype of the UCI laboratory). Inter-comparison experiments were undertaken between these two analytical systems, and the chemical analysis results were comparable (as described in Text S2).

In addition, the trace gas carbon monoxide (CO) was simultaneously monitored during most sampling campaigns using a gas filter correlation trace level CO analyzer (API model 300EU) coupled with a heated, platinum CO scrubber. The quality assurance and quality control of CO measurement are described in detail in Text S3.

2.3 PMF Receptor Model

The source changes of halocarbons between 2001 and 2018 in the Greater PRD region were identified using the Positive Matrix Factorization (PMF) 5.0 model. In this model, based on the composition or fingerprints of the sources, a mathematical method is applied to determine the contribution of sources to samples. An air sampling data set can be regarded as a data matrix x of i by j dimensions. The chemical mass balance between measured species concentrations and source profiles can be described as follows (Equation (1)):

$$x_{ij} = \sum_{k=1}^{p} g_{ik} f_{kj} + e_{ij} \quad (1)$$

where x_{ij} is the mixing ratio *of* jth species in the ith sample, g_{ik} is the proportion of the kth source to ith sample, f_{kj} is the fraction of the jth species in the kth source, e_{ij} is the residual value for the jth species in the ith sample, and p is the total number of independent sources [*Paatero*, 1997].

As a multivariable factor analysis program, PMF resolves a matrix of sample data into two matrices: factor contributions (G) and factor profiles (F). The various sources that may contribute to the samples are determined according to the extracted factor profiles. For all chemical species (m) in all the samples (n), factor contributions and profiles are obtained from the model minimizing the objective function Q (Equation (2)):

$$Q = \sum_{i=1}^{m} \sum_{j=1}^{n} \left[\frac{x_{ij} - \sum_{k=1}^{p} g_{ik} f_{kj}}{u_{ij}} \right]^2 \quad (2)$$

where u_{ij} is an estimate of the ‘‘uncertainty’’ in the jth species in the ith sample, which is determined by the equation u = 5/6 × method detection limit (MDL) when the concentration is ≤the MDL value; or by u = [(error fraction × mixing ratios)^2 + (MDL)^2]$^{1/2}$ when the concentration is > MDL value [*Paatero*, 1997; *Zhang et al.*, 2014].

To better understand the sources of halocarbons, the source contributions, and the source changes in the past 18 years in the Greater PRD region, source apportionment was conducted on the whole dataset using PMF v5.0. Ten main halocarbons (as shown in section 3.3) were used for the model simulation as they had relatively high ambient mixing ratios and are typical tracers of various emission sources. They were also available in most years except 2007 and 2010. In addition, as a combustion tracer, CO was an input for model simulation. In total, 934 valid samples were used as inputs for source apportionment, and the uncertainty of the input species was set as 10%.

2.4 Emission Estimation

Previous studies have indicated that the ratios between the enhancements of halocarbons and a tracer can demonstrate their emission strengths. The selection of the tracer should follow the following rules: (1) a long lifetime and low chemical reactivity occurred during the transport; (2) known emissions; and (3) correlation with halocarbons that is as good as possible. Carbon monoxide (CO) is often chosen as the tracer to determine the halocarbon emissions [*Palmer et al.*, 2003; *Guo et al.*, 2009]. Although the sources of halocarbons and CO are not exactly the same, their sources are often co-located, such as coexisted refrigeration and combustion in factories, vehicles and households. Moreover, similar to halocarbons, CO has a relatively long lifetime and is less reactive, and the emission inventory of CO is more easily accessible than other species. Hence, the ratio of halocarbon species to CO has been widely used to estimate the emissions of halocarbons [*Palmer et al.*, 2003; *Guo et al.*, 2009; *Shao et al.*, 2011; *Fang et al.*, 2012; *Wang et al.*, 2014]. In this study, we used CO as the reference compound to estimate the halocarbon emissions in the Greater PRD region in 2016 as an example.

The emission of each halocarbon can be calculated by Equation (3) [*Shao et al.*, 2011]:

$$E_X = E_{CO} \times R \times \frac{M_X}{M_{CO}} \tag{3}$$

where E_X and E_{CO} are the emissions of the halocarbon X and CO, respectively; R is the slope of the linear correlation between the enhancements of halocarbon and CO (Δhalocarbon and ΔCO), which are obtained by subtracting the background values, especially for long-term observations. In this study, background values were defined as the lowest 20th percentile of the complete datasets for each halocarbon. The lowest CO mixing ratio in South China Sea air (defined by backward trajectory simulation) was characterized as the CO background value [*Shao et al.*, 2011]. Halocarbon emissions in 2016 were estimated, when samples were mainly collected in autumn (October and November). Under similar synoptic conditions within this short period, the background value was supposed to change insignificantly. Since the emission estimation was based on the slopes of correlations between the species, whether the background value was subtracted or not would not influence the results [*Shao et al.*, 2011; *Fang et al.*, 2012]. M_X and M_{CO} are the molecular weights of the halocarbon X and CO, respectively.

Using linear least squares fitting method, the uncertainties of halocarbon emissions can be estimated by Equation (4) [*Shao et al.*, 2011]:

$$\sigma_x = \sqrt{\sigma_{E_{CO}}^2 \times R^2 + E_{CO}^2 \times \sigma_R^2} \times \frac{M_x}{M_{CO}} \quad (4)$$

where σ_x is the uncertainty of the estimated halocarbon emission, $\sigma_{E_{CO}}$ and σ_R are the uncertainties of E_{CO} and R, respectively.

3. Results and Discussion

3.1 General Features

Table 2 summarizes the mean mixing ratios (with 95% confidence level) of 15 halocarbons in the Greater PRD (subtropical climate in the Northern Hemisphere (NH)), which are compared with the levels at the Mauna Loa station (MLO), Hawaii (19.54°N, 155.58°W) from 2001 to 2018 [*ESRL*, 2018]. The reason for choosing MLO site was that it provided a complete data set for the study period and is representative of NH subtropical background levels of halocarbons. Average mixing ratios of halocarbons in the Greater PRD were calculated in four sampling periods (I: 2001-2004, II: 2005-2008, III: 2010-2013, and IV: 2015-2018), which mainly reflected the temporal variations of halocarbons in this region. Moreover, backward trajectories were simulated on individual sampling days and origins of air masses were clustered into four categories (Figure S2). Categories 2 and 3 came from the northeast of the Greater PRD region, passing by relatively clean coastal areas. Remarkably, under the influence of the background of the South China continent, air masses in these two categories (82%) stayed in Guangdong province for more than 24 hrs before reaching the study region, representative of local characteristics. Hence, categories 2 and 3 were further analyzed while categories 1 (super-regional) and 4 (oceanic) were excluded.

Among all measured halocarbons (Table 2), the average value of CH_3Cl was the highest, followed by CH_2Cl_2, CFC-12 and HCFC-22, indicating large-scale emissions of these species from various sources in the study region. In comparison, the averages of halocarbons for the whole period in the Greater PRD region were all higher ($p < 0.05$) than the tropical NH background values at the MLO site, consistent with our previous findings [*Guo et al.*, 2009; *Zhang et al.*, 2010b]. Specifically, mixing ratios of HCFC-22, H-1211, HFC-134a, CH_3Cl, CH_3CCl_3 and CH_3Br were approximately twice those at the MLO site. Moreover, abundances of CH_2Cl_2 and C_2Cl_4 in the study region were 25 and 50 times those at MLO site. The results indicated significant contributions of local emissions (including "bank" emissions) and perhaps unreported new production [*SPARC*, 2017; *Lunt et al.*, 2018; *Montzka et al.*, 2018].

Inspection on the averages of CFC-113, H-1211 and CCl_4 in different periods found their continuous decrease ($p<0.005$), implying the effectiveness of the Montreal Protocol regulations on these species. In addition, values of other CFCs, *i.e.* CFC-11 and CFC-12, declined ($p<0.005$) from period III to period IV. Their levels in period III were similar to the results of a study conducted in 2010 in this region [*Wu et al.*, 2013]. Similarly, C_2Cl_4, CH_2Cl_2 and $CHCl_3$ experienced obvious decline ($p<0.005$) from periods III to IV. In contrast, as substitutes of phased-out CFCs, HCFC-22 and HFC-134a had the highest averages in period IV compared to previous periods, reflecting their expanding productions in this region. Besides, similar levels of HCFC-22 (526 pptv, 69% as relative standard deviation) and HFC-134a (84 pptv, 48%) were reported in suburban Guangzhou, 2010 [*Wu et al.*, 2013]. As the most abundant species, CH_3Cl experienced an increase ($p<0.05$) from periods I to III, and remained unchanged in periods III and IV, reflecting a possible alleviation in its increase.

3.2 Long-term Temporal Variations of Halocarbons in the Greater PRD Region

To evaluate the implementation status of halocarbon control measures, it is crucial to know the long-term changes of halocarbons. Although the halocarbon data were not continuously measured at a fixed site in this study, it was still possible to infer the variation trends of halocarbons in these years if we integrated and analyzed a range of halocarbon levels at some rural or suburban sites with similar sources and geographical environments. Figure 2 presents the trends of monthly averages of fifteen key halocarbons in the Greater PRD region from 2001 to 2018, compared with the monthly average mixing ratios of eleven halocarbons at MLO with error bars (95% confidence interval) during the same period. It should be noted that error bars are provided for our measurement data whenever more than one sample was collected per month (Figure 2). The dashed lines are the linear fits to the halocarbon mixing ratios [*Kock et al.*, 2005; *Qin et al.*, 2007; *Zhang et al.*, 2010a; *Zhang et al.*, 2010c]. Please note: the variation rates of some species may not be exactly constant during the whole period due to different control regulations. However, the linear regression method can provide reliable average variation trends throughout the 18 years. Moderate to good R^2 of regressions were obtained for most halocarbons. The slope of each halocarbon represented the yearly variation rate of each halocarbon (Figure 2). For easy comparison, the yearly growth rates of target halocarbons in the Greater PRD region and at the MLO site are summarized in Table 3.

Overall, the monthly averages of all halocarbons in the Greater PRD region were higher than the corresponding NH background levels, revealing the contribution of anthropogenic activities to these halocarbons (Figure 2). However, the error bars of some species, *i.e.* CFC-11 and CFC-12, sometimes reached the levels lower than the background values, perhaps caused by the discrepancy between our offline analytical system and the online system at MLO site.

Table 2 Mixing Ratios of Halocarbons in the Greater PRD Region in Different Periods, Together With Subtropical Northern Hemisphere Background Levels from NOAA (Units: pptv)

Compounds (Chemical Formula)	MLO Background Mean[a] (95% CI)[b]	Average (±95% CI)[b] in the Greater PRD				
	Whole period	Whole period	2001-2004	2005-2008	2010-2013	2015-2018
CFC-11 (CCl_3F)	242±1.3	270±1.7	292±1.7	249±4.8	261±2.0	245±5.3
CFC-12 (CCl_2F_2)	530±1.6	571±42.9	603±3.2	569±9.7	571±3.3	508±6.6
CFC-113 (CCl_2FCClF_2)	78±0.5	88±1.0	97±1.3	90±2.2	85±0.7	66±3.8
CFC-114 ($CClF_2CClF_2$)		17±0.16	16±0.1	16±0.4	17±0.2	20±0.5
HCFC-22 ($CHClF_2$)	204±2.1	398±11	281±8.8	502±36	379±17	625±33
H-1211 (CF_2ClBr)	4.1±0.04	9.2±0.47	13±0.7		5.6±0.2	3.9±0.3
HFC-134a (CH_2FCF_3)	58±1.7	113±7.1	61±7.2		80±3.3	230±13
Methyl chloride (CH_3Cl)	555±4.2	1036±17	910±15	1059±45	1102±26	1171±63
Carbon tetrachloride (CCl_4)	90±0.8	108±1.1	121±1.2	112±2.7	97±1.1	89±1.9
Methyl Chloroform(CH_3CCl_3)	13±1.5	32±1.7	60±2.6	37±3.4	7.0±0.2	5.9±1.2
Tetrachloroethene(C_2Cl_4)	1.7±0.04	85±5.2	121±11	79±12	65±5.9	43±3.9
Methylene chloride (CH_2Cl_2)	39±1.1	960±53	826±73		1132±117	821±59
Methyl bromide (CH_3Br)	7.7±0.05	18±0.43	16±0.5	25±1.4	17±0.9	17±0.8
Chloroform ($CHCl_3$)		59±2.4	45±2.4	178±16	78±4.3	43±3.3
Methyl iodide (CH_3I)		2.3±0.20	2.0±0.1		1.7±0.1	3.3±0.8

a. Subtropical NH background value from the NOAA/ESRL halocarbons program, https://www.esrl.noaa.gov/gmd/dv/data/index.php?category=Halocompounds. The monthly mean values at Mauna Loa, Hawaii from 2001 to 2018 are used. Measured in pptv; b. 95% CI represents 95% confidence interval.

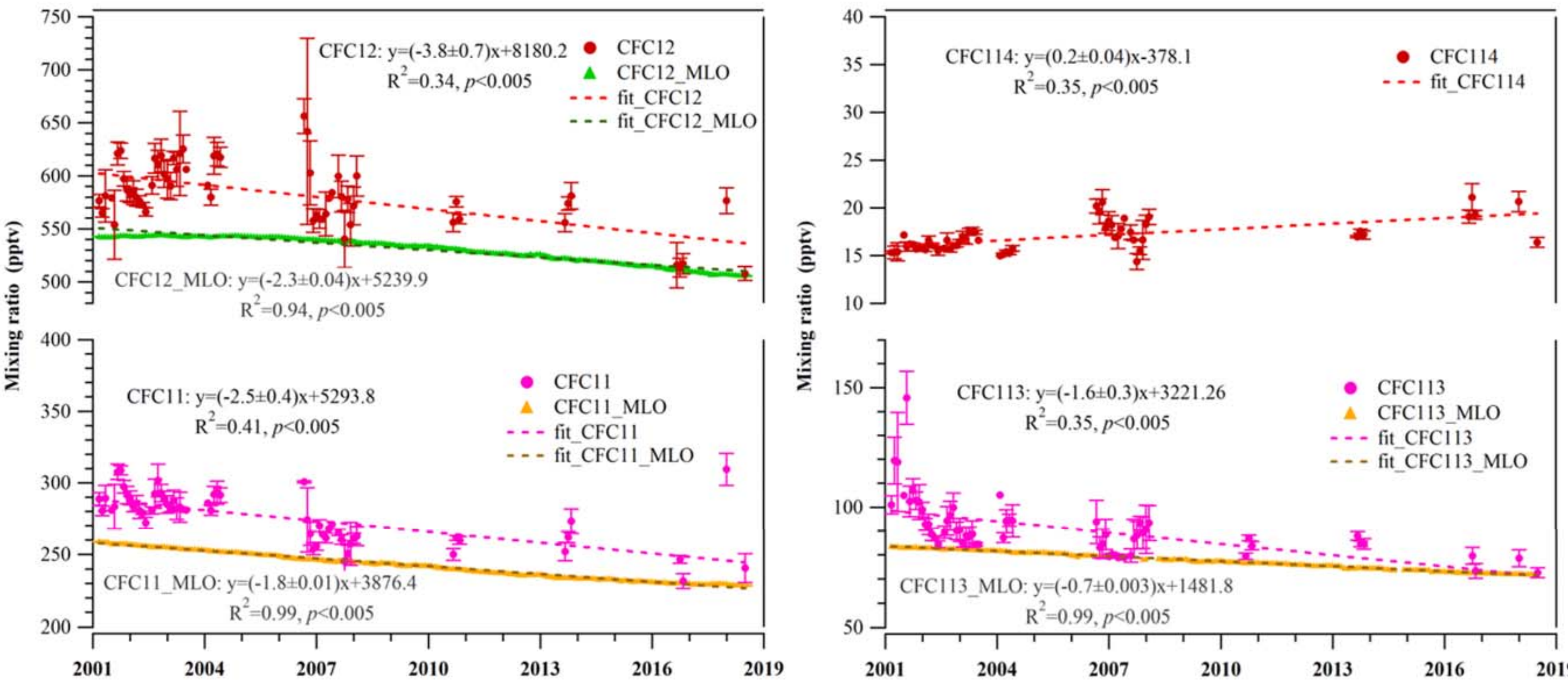

CFC12: y=(-3.8±0.7)x+8180.2
R^2=0.34, p<0.005
CFC12
CFC12_MLO
fit_CFC12
fit_CFC12_MLO
CFC12_MLO: y=(-2.3±0.04)x+5239.9
R^2=0.94, p<0.005
CFC11: y=(-2.5±0.4)x+5293.8
R^2=0.41, p<0.005
CFC11
CFC11_MLO
fit_CFC11
fit_CFC11_MLO
CFC11_MLO: y=(-1.8±0.01)x+3876.4
R^2=0.99, p<0.005
CFC114: y=(0.2±0.04)x-378.1
R^2=0.35, p<0.005
CFC114
fit_CFC114
CFC113: y=(-1.6±0.3)x+3221.26
R^2=0.35, p<0.005
CFC113
CFC113_MLO
fit_CFC113
fit_CFC113_MLO
CFC113_MLO: y=(-0.7±0.003)x+1481.8
R^2=0.99, p<0.005
Mixing ratio (pptv)
Mixing ratio (pptv)
750
700
650
600
550
500
400
350
300
250
200
40
35
30
25
20
15
10
150
100
50
2001
2004
2007
2010
2013
2016
2019
2001
2004
2007
2010
2013
2016
2019

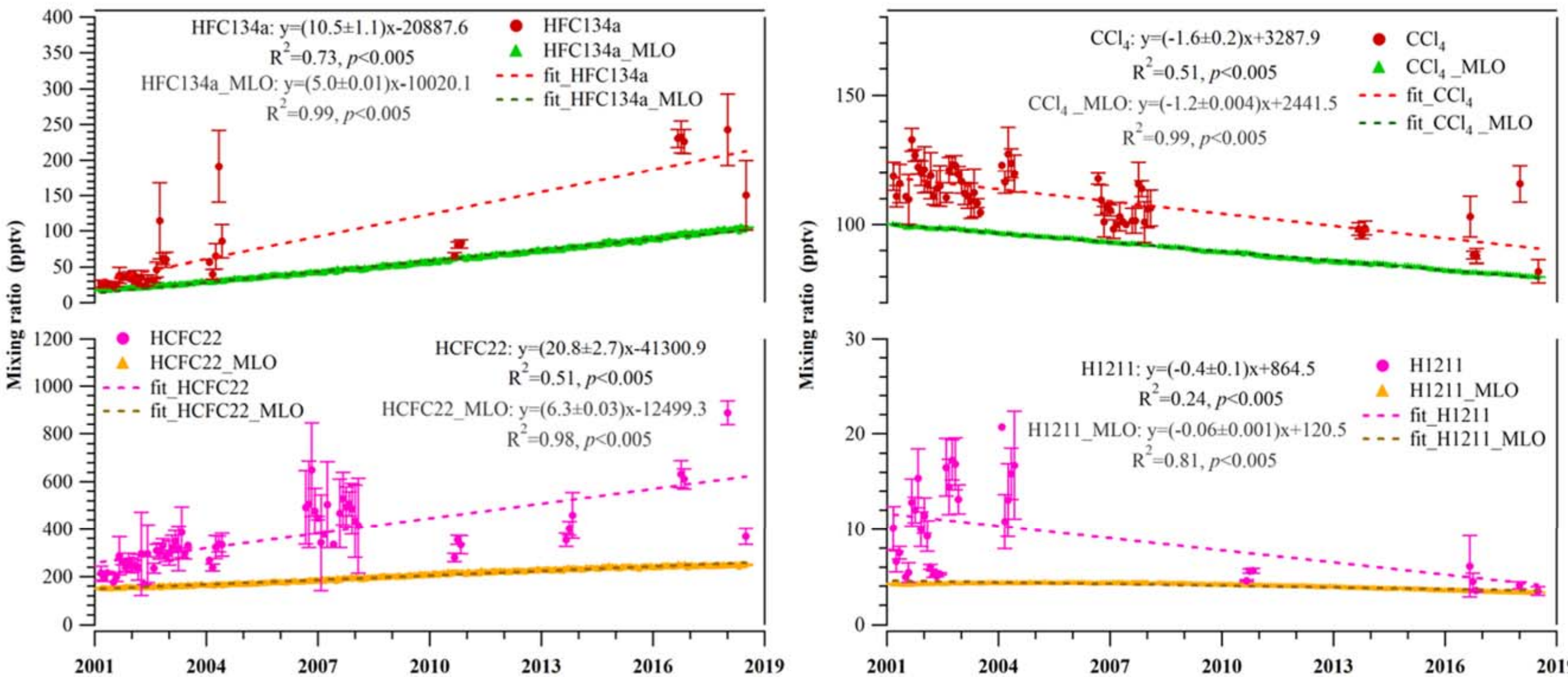

HFC134a: y=(10.5±1.1)x-20887.6
R2=0.73, p<0.005
HFC134a_MLO: y=(5.0±0.01)x-10020.1
R2=0.99, p<0.005
HFC134a
HFC134a_MLO
fit_HFC134a
fit_HFC134a_MLO
CCl4: y=(-1.6±0.2)x+3287.9
R2=0.51, p<0.005
CCl4_MLO: y=(-1.2±0.004)x+2441.5
R2=0.99, p<0.005
CCl4
CCl4_MLO
fit_CCl4
fit_CCl4_MLO
HCFC22
HCFC22_MLO
fit_HCFC22
fit_HCFC22_MLO
HCFC22: y=(20.8±2.7)x-41300.9
R2=0.51, p<0.005
HCFC22_MLO: y=(6.3±0.03)x-12499.3
R2=0.98, p<0.005
H1211: y=(-0.4±0.1)x+864.5
R2=0.24, p<0.005
H1211_MLO: y=(-0.06±0.001)x+120.5
R2=0.81, p<0.005
H1211
H1211_MLO
fit_H1211
fit_H1211_MLO
Mixing ratio (pptv)
Mixing ratio (pptv)
2001
2004
2007
2010
2013
2016
2019
2001
2004
2007
2010
2013
2016
2019

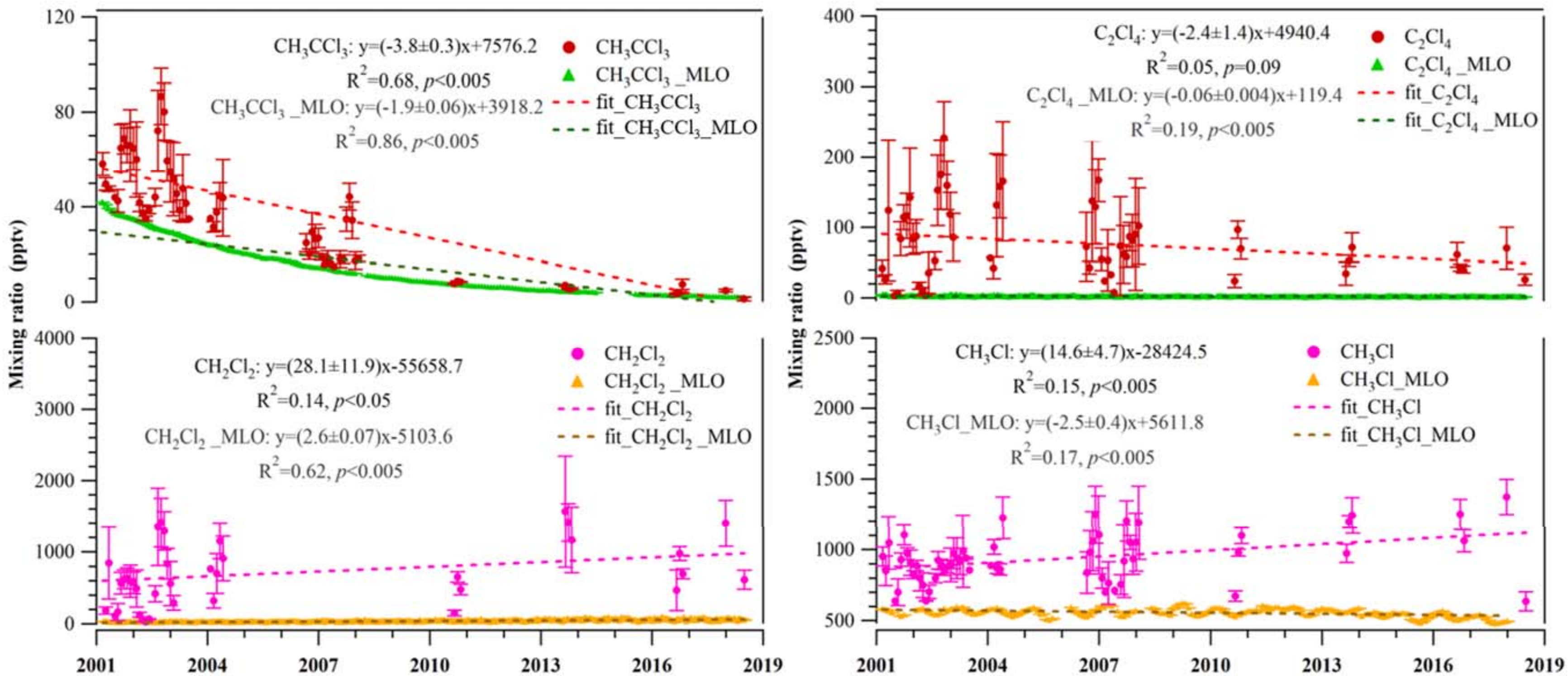

CH_3CCl_3: y=(-3.8±0.3)x+7576.2
R^2=0.68, p<0.005
CH_3CCl_3 _MLO: y=(-1.9±0.06)x+3918.2
R^2=0.86, p<0.005
CH_3CCl_3
CH_3CCl_3 _MLO
fit_CH_3CCl_3
fit_CH_3CCl_3_MLO
C_2Cl_4: y=(-2.4±1.4)x+4940.4
R^2=0.05, p=0.09
C_2Cl_4 _MLO: y=(-0.06±0.004)x+119.4
R^2=0.19, p<0.005
C_2Cl_4
C_2Cl_4 _MLO
fit_C_2Cl_4
fit_C_2Cl_4 _MLO
CH_2Cl_2: y=(28.1±11.9)x-55658.7
R^2=0.14, p<0.05
CH_2Cl_2 _MLO: y=(2.6±0.07)x-5103.6
R^2=0.62, p<0.005
CH_2Cl_2
CH_2Cl_2 _MLO
fit_CH_2Cl_2
fit_CH_2Cl_2 _MLO
CH_3Cl: y=(14.6±4.7)x-28424.5
R^2=0.15, p<0.005
CH_3Cl_MLO: y=(-2.5±0.4)x+5611.8
R^2=0.17, p<0.005
CH_3Cl
CH_3Cl_MLO
fit_CH_3Cl
fit_CH_3Cl_MLO
Mixing ratio (pptv)
2001 2004 2007 2010 2013 2016 2019

358

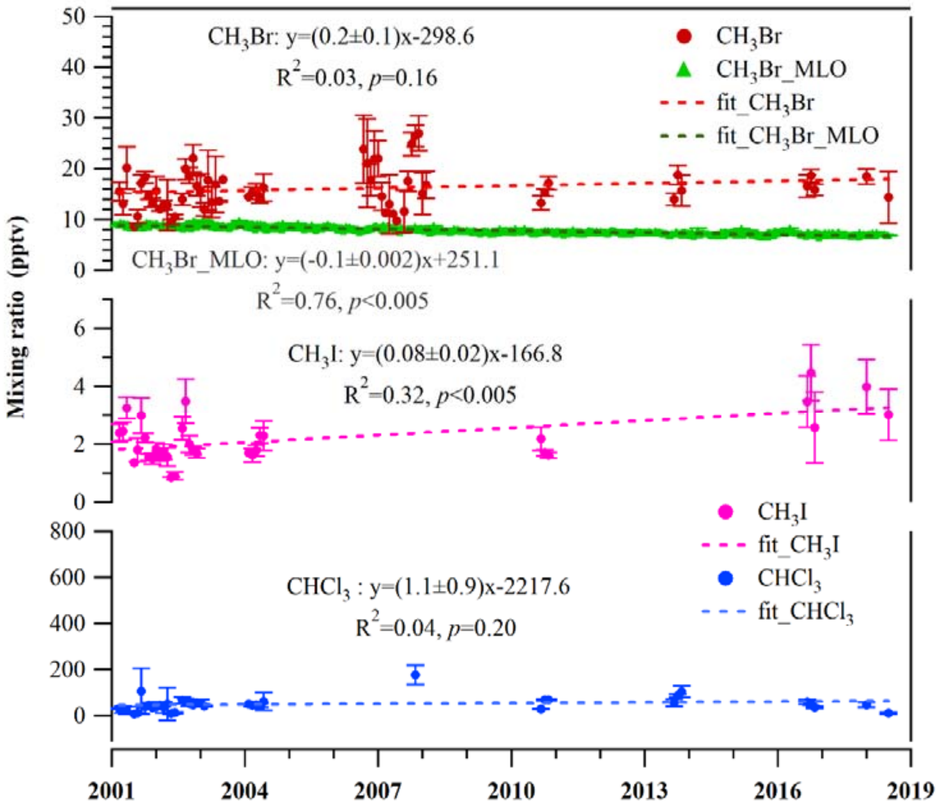

Figure 2 Monthly Variations of Halocarbons in the Greater PRD from 2001 to 2018.

Specifically, the mixing ratios of CFC-11, CFC-12, CFC-113 and H-1211 showed significant (p<0.005) decreasing trends (-2.5±0.4, -3.8±0.7, -1.6±0.3, -0.4±0.1 pptv/yr) while CFC-114 presented a small long-term increase (0.2±0.04 pptv/yr, p<0.005). The increasing pattern of CFC-114 was different from the global level which exhibited a slower declining trend in 2012-2016 compared to 2008-2012 [*WMO/UNEP*, 2018], but was similar to the findings of recent studies which indicated significant emissions of CFC-114 in East Asia (probably in Mainland China) in 2012-2016 [*Laube et al.*, 2016; *Vollmer et al.*, 2018]. Similar declining trends for CFC-11, CFC-112 and H-1211 from 1998 to 2008 were reported in this region (both HK and the inner PRD) in previous study [*Zhang et al.*, 2010b]. Moreover, the decreasing rates of CFC-11, CFC-12, CFC-113 and H-1211 in the Greater PRD region were all higher than those at the MLO site (Table 3), indicating an efficient control under phase-out policies for CFCs and halons in South China. What's more, the mixing ratios of CFC-12, CFC-113 and H-1211 almost reached the NH background levels at MLO after 2016, while an increased emission of CFC-11 proposed in East Asia was likely responsible for the relatively slower decline of CFC-11 after 2012 [*Montzka et al.*, 2018], which also explained the larger difference in mixing ratio of CFC-11 between the Greater PRD region and the MLO site in recent years, compared to the other three species mentioned above.

In contrast, the levels of HCFC-22 and HFC-134a in the Greater PRD region increased (p<0.05) during the past 18 years. As shown in Figure 2 and Table 3, the annual growth rate of HCFC-22 (20.8±2.7 pptv/yr) was triple that at MLO site (6.3±0.03 pptv/yr), revealing continuous urban emissions. The production of HCFC-22 in 2010 and 2014 in China was 522 kt and 597.7 kt, respectively, while Hong Kong, as a "non-Article 5" party, has to reduce 90% HCFCs consumption by 2015 and 100% by 2030, indicating great challenges in managing its emissions over the next decade [*CFOMIA*, 2016]. The growth rate of HFC-134a (10.5±1.1 pptv/yr) was twice that of the NH background (5.0±0.01 pptv/yr). Because of similar thermodynamic properties to CFC-12, an insignificant ODP and a low global warming potential, HFC-134a is nowadays a substitute of CFC-12 [*Su et al.*, 2015]. In China, the HFC-134a production in 2014 almost doubled (162.3 kt) compared to that in 2010 (83.6 kt) [*CFOMIA*, 2016]. In summary, more reduction efforts are needed to mitigate the increase in the production and consumption of the alternative HCFCs and even HFCs after the ban of CFCs use in China.

Similar to CFC-11 and CFC-12, the CCl_4 mixing ratios decreased (p<0.005) at a rate of -1.6±0.2 pptv/yr from 2001 to 2018, more rapidly than that at the MLO background site (-1.2±0.004 pptv/yr). Moreover, CH_3CCl_3 declined from 2001 to 2018 at a rate of -3.8±0.3 pptv/yr, which was twice that NH subtropical background level (-1.9±0.06 pptv/yr). *Xue et al.* [2011] also reported the continuing declines in the ambient mixing ratios of CCl_4 and CH_3CCl_3 in northeast China. Furthermore, the monthly average mixing ratios of CH_3CCl_3 almost reached the NH subtropical background levels after 2016, suggesting an effective reduction of this solvent species in this region. However, the mixing ratio of C_2Cl_4 experienced a slight decrease but without significance (p=0.09) in the Greater PRD region despite its continuous reduction at MLO, indicating its continuous use, mainly as dry cleaning agent and degreasing fluid in the Greater PRD region.

Methyl chloride (CH_3Cl), the most abundant halocarbon in this study, increased (p<0.005) at a rate of 14.6±4.7 pptv/yr from 2001 to 2018, though it decreased significantly at MLO (-2.5±0.4 pptv/yr), implying the un-controlled emissions of some CH_3Cl sources, such as the use of solvent (including degreasant, oil paint and binding agent), oceanic emissions and biomass burning activities [*Guo et al.*, 2009]. Our previous study indicated that CH_3Cl was mainly emitted from the refrigeration industry and biomass/biofuel burning in the PRD region [*Guo et al.*, 2009]. The exact causes for its increased growth rate in these years remain unknown. Source apportionment in the following section might give some hints.

Furthermore, CH_2Cl_2 was the fastest-growing halocarbon with a growth rate of 28.1±11.9 pptv/yr, while its NH subtropical background growth rate was only 2.6±0.07 pptv/yr. Similarly, growth in CH_2Cl_2 was captured in all NH regions between 1998 and 2012 [*Leedham Elvidge et al.*, 2015]. Increased CH_2Cl_2 levels were likely attributable to the increased solvent consumption in the Greater PRD region. In addition, the mixing ratio of $CHCl_3$ remained invariable in the past 18 years, different from the increase in eastern China (increased by 49 (41-59) Gg between 2010 and 2015) but similar to the insignificant change in southern China from 2007 to 2015 [*Fang et al.*, 2019]. $CHCl_3$ is mostly used as a feedstock to produce HCFC-22, tetrafluoroethene and Teflon, with a limited use as an extractant for pharmaceutical products [*Rossberg et al.*, 2011].

The increase of CH_3Br from 2001 to 2018 was insignificant (p=0.16), while CH_3I showed an increasing trend at 0.08±0.02 pptv/yr (p<0.005). Sources of CH_3Br include use as a fumigant and as a leaded fuel additive, oceanic production, biomass burning, and plant and marsh emissions [*Seinfeld and Pandis*, 2016], but the anthropogenic uses of CH_3Br have been prohibited in this region [*CHP*, 2018; *HKEPD*, 2018a; *Vollmer et al.*, 2009; *Wang et al.*, 2006]. Hence, natural sources, *i.e.* biomass burning and oceanic emissions, are the most likely sources of CH_3Br. *WMO/UNEP* [2018] reported that global natural sources of CH_3Br remained at a constant level from 1996 to 2016, in agreement with the invariable trends in this study. CH_3I is known as an important tracer of oceanic emissions [*Lennartz et al.*, 2015] and was found over the Tropical Western Pacific [*Fuhlbrugge et al.*, 2016] and the Indian Ocean [*Fiehn et al.*, 2017]. *Rasmussen et al.* [1982] also found that near-oceanic regions characterized by high biomass productivity could yield 10 - 20 pptv of CH_3I. Besides, CH_3I is used as methylating agents [*Yin et al.*, 2014]. In comparison, *Yokouchi et al.* [2012] claimed the varied trends of CH_3I over the past decades, while the best estimate reported by *Carpenter and Reimann et al.* [2014] indicated no changes in CH_3I from coastal and open-oceans emissions. Thus, the growth of CH_3I was more possibly attributed to anthropogenic activities. Further investigation is necessary.

Given that the long-term measurement data of halocarbons at a fixed site were not available in this study, we integrated several field measurements of halocarbons conducted in the past 18 years at rural and/or suburban sites with similar geographical proximity to study the long-term variations of halocarbons. Even so, this method might have some uncertainties, such as representative error, meteorological impact and instrumental error. We selected the halocarbon datasets collected at geographically similar sites to minimize the representative error. For the instrumental error, we used the same protocols of air sampling, the same chemical standards for analysis, and the same instrumental calibration and analytical method throughout the whole period. For the samples analyzed in our laboratory, we followed the same procedures as those in the Rowland/Blake laboratory, and frequently carried out inter-comparison between the two laboratories to guarantee the data quality. Besides, the meteorological impact was partially considered during the data analysis by removing samples under the influence of oceanic and super-regional air masses from the whole dataset. Moreover, the influence of data collected at each sampling site and in individual years, especially those years with obvious step changes in mixing ratio, on the long-term trends was assessed via comparison of scenarios of including and excluding data at a specific site and in a specific year. The impact of various sites and different years on the variation rates are listed in Tables S2 and S3, respectively (described in Text S4). In addition, standard errors for all variation rates were presented to reflect the variability and reliability of the results (Figure 2 and Table 3). Overall, despite some uncertainties, the precious long-term halocarbon data could still provide useful information on temporal variations of halocarbons to infer the implementation of the Montreal Protocol in the Greater PRD region.

Table 3. Annual Growth Rate of Halocarbons in the Greater PRD region and at the MLO Site

Compounds (Chemical Formula)	Annual growth rate in the Greater PRD (2001-2018) (pptv/yr)	Annual growth rate at MLO (2001-2018) (pptv/yr)
CFC-11 (CCl_3F)	-2.5±0.4	-1.8±0.01
CFC-12 (CCl_2F_2)	-3.8±0.7	-2.3±0.04
CFC-113 (CCl_2FCClF_2)	-1.6±0.3	-0.7±0.003
CFC-114 ($CClF_2CClF_2$)	0.2±0.04	-
HCFC-22 ($CHClF_2$)	20.8±2.7	6.3±0.03
H-1211 (CF_2ClBr)	-0.4±0.1	-0.06±0.001
HFC-134a (CH_2FCF_3)	10.5±1.1	5.0±0.01
Methyl chloride (CH_3Cl)	14.6±4.7	-2.5±0.4
Carbon tetrachloride (CCl_4)	-1.6±0.2	-1.2±0.004
Methyl Chloroform(CH_3CCl_3)	-3.8±0.3	-1.9±0.06
Tetrachloroethene(C_2Cl_4)	-2.4±1.4[#]	-0.06±0.004
Methylene chloride (CH_2Cl_2)	28.1±11.9	2.6±0.07
Methyl bromide (CH_3Br)	0.2±0.1[#]	-0.1±0.002
Chloroform ($CHCl_3$)	1.1±0.8[#]	-
Methyl iodide (CH_3I)	0.08±0.02	-

#. Non-significant, $p>0.05$.

3.3 Emission Source Profiles in the Greater PRD region

Figure 3 shows the source profiles resolved from the PMF modeling. Six sources were identified in the Greater PRD region. The first source (F1) was distinguished by high percentages of CFCs, such as CFC-11 (61.2±1.1 %), CFC-12 (63.7±2.0 %), CFC-113 (53.9±1.3 %) and CFC-114 (62.6±1.5 %). CFCs are mainly used as refrigerants in air conditioning systems and cooling appliances. Unlike other CFCs, CFC-11 is not only a refrigerant, but also extensively used as aerosol-spray propellants, foam-blowing agents and solvents in the air conditioning systems in South China [*Chan et al.*, 2006b]. Though CFC-11 has various applications, these uses are mostly related to the cooling appliances. Thus these CFC species were grouped under the same factor. Moreover, this factor explained 54.5±1.2 % of CCl_4. Prior to the Montreal Protocol, large quantities of CCl_4 were used to produce CFC-11 and CFC-12 [*Simmonds et al.*, 1998]. CH_3Cl also showed a high percentage (44.7±2.5 %), because it was once used as a refrigerant (R-40) [*Sikdar*, 2001]. *Zhang et al.* [2010b] and *Guo et al.* [2009] also found that CCl_4 and CH_3Cl had high correlations with CFCs in the PRD region. Interestingly, 37.9±0.8 % of HCFC-22 was quantified in this factor. HCFC-22 has been largely used as refrigerants after the phase-out of CFCs, which might co-locate with CFCs. Overall, the profile was consistent with previous studies in South China [*Guo et al.*, 2009; *Zhang et al.*, 2010b]. Hence, this source was categorized as the refrigeration industry.

A high mass percentage of HCFC-22 (60.4±2.5 %) was observed in the second factor (F2), with low loadings of other tracers. Being a replacement of CFCs, HCFC-22 is mainly used in household and commercial refrigeration equipment and its emission grew rapidly after the prohibition of CFCs. Thus we considered this source as the replacement of CFCs.

The third source (F3) was inferred as solvent use in the electronic industry and dry cleaning, characterized by high percentage of C_2Cl_4 (78.6±2.2 %). C_2Cl_4 is primarily used as an industrial cleaning solvent, metal degreasing agent and dry cleaning fluid [*Simmonds et al.*, 2006]. In the study region, many dry cleaners spread in the urban areas and some electronic workshops reside in industrial areas [*Guo et al.*, 2009; *Zhang et al.*, 2010b]. This factor also accounted for 27.9±1.1 % of CFC-113, since CFC-113 is often used as a solvent in electronic industry. However, the contribution of this factor to CFC-113 was lower than that in 2001-2002 reported by *Guo et al.* [2009]. This was attributed to the successful replacement of CFC-113 in electronic industry after the implementation of Montreal Protocol [*Chang et al.*, 2008].

The fourth source (F4) was industrial and domestic solvent use, characterized by high percentages of CH_2Cl_2 (86.0±2.2 %). Because of its volatility and ability to dissolve a wide range of organic compounds, CH_2Cl_2 is predominantly used as a solvent, such as paint stripper, spray fluid, release agent, and cleaning solvent [*Borkar et al.*, 2010].

The fifth factor (F5) was considered to be feedstock in chemical manufacturing. High contribution of $CHCl_3$ (85.7±4.3 %) was found and other halocarbons made negligible contributions to this source. As an important feedstock, the most important use of $CHCl_3$ is the reaction with hydrogen fluoride to produce HCFC-22, largely for air conditioning applications and the production of polytetrafluoroethylene (Teflon) [*Rossberg et al.*, 2011].

The last source (F6) was characterized by high loading of CO (80.2±2.5 %), indicating its association with combustion sources. Further, 27.1±2.3 % of CH_3Cl was found in this source. Indeed, biomass/biofuel burning is one of the CH_3Cl sources and was identified in previous studies including studies in the PRD region [*Thompson et al.*, 2002; *Guo et al.*, 2009; *Zhang et al.*, 2010b]. As such, this source was influenced by biomass burning and/or coal burning.

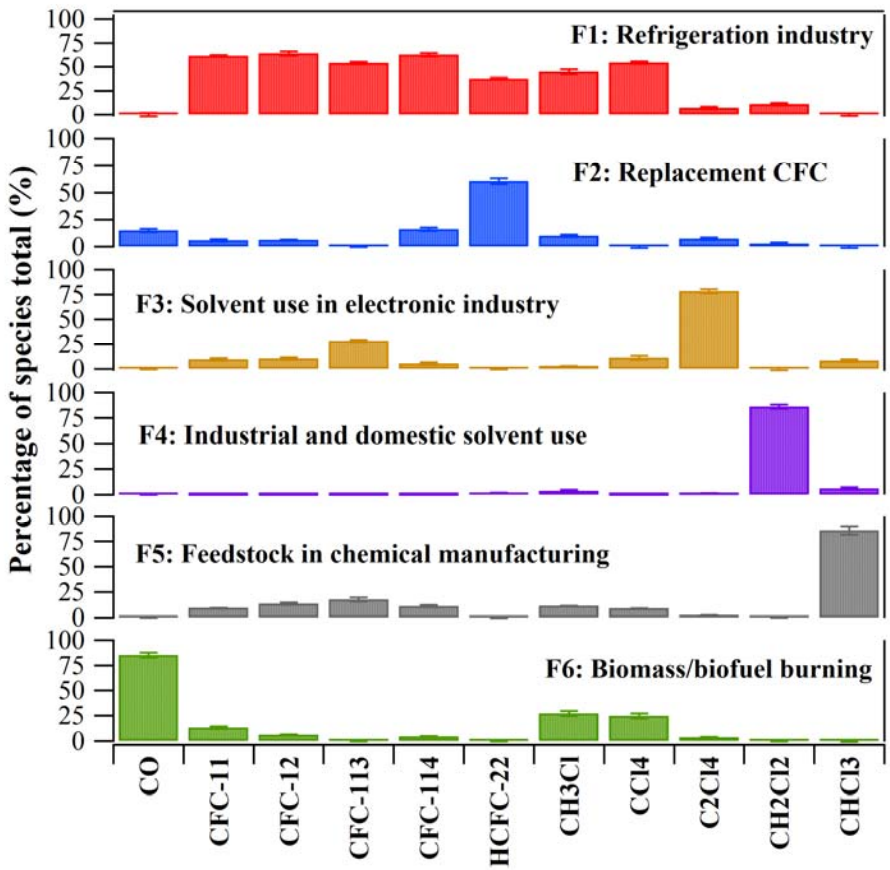

Figure 3. Source Profiles Resolved from PMF in the Greater PRD region

3.4 Temporal Variations of Halocarbon sources in the Greater PRD region

Temporal variations of source contributions to halocarbons in the Greater PRD region were extracted from the PMF results and merged into individual years, as shown in Figure 4 (in mixing ratio) and Figure S3 (in percentage). Two refrigeration application-related sources showed reverse trends in mixing ratios and in percentages during the study period. The refrigeration industry source dominated by CFCs experienced a progressive decline in the contribution to total halocarbons, from 1638.4±35.4 pptv (52.2±2.8%) in 2001 to 1167.1±60.9 pptv (34.5±2.4%) in 2018. CH_3Cl in this source decreased from ~540 pptv (~61%) in 2001 to ~400 pptv (~40%) in 2018. During the whole study period, source of refrigeration industry was always the largest contributor to the ten input halocarbons. In contrast, the contribution of replacement of CFCs, whether it is in mixing ratio or percentage, continued to increase from 197.1±13.1 pptv (6.3±0.5%) in 2001 to 848.1±180.8 pptv (25.1±2.2%) in 2018. The source of replacement of CFCs contributed only 6.3±0.5 – 12.4±0.6% during 2001-2013, while it became the second largest contributor to total halocarbons after 2016 with percentages of 22.7±1.0 – 25.1±2.2%, revealing successful replacement of CFCs with HCFC-22 in the Greater PRD region. Since the production and consumption of CFCs has been banned after mid-2007 in China (in 1996 in HK), the largest contribution of refrigeration industry in recent years to halocarbons was possibly attributed to background level and/or leakage from existing products or landfills.

Solvent use in electronic industry traced by C_2Cl_4 decreased dramatically from 358.6±51.0 – 509.8±111.4 pptv (11.4±1.6 – 14.9±1.4%) during 2001-2004, to 209.3±27.6 pptv (5.7±0.4%) in 2013, and remained at a low level of 162.6±58.5 – 167.5±20.3 pptv (4.8±1.1 – 5.3±0.5%) during 2016-2018. This result confirmed the effective control of solvent use (mainly C_2Cl_4) in electronic industry in this region. The other three sources, including industrial/domestic solvent use, feedstock in chemical manufacturing and biomass/biofuel burning, were invariable during the study period. In southern China, forest fires and cropland fires were two main sources of biomass burning. *Yin et al.* [2019] estimated a decreased emission of forest fire but an increase in the emission of cropland fire from 2003 to 2017. Total biomass burning emission in China decreased remarkably in 2015-2016, but bounced in 2017. The insignificant variation of biomass burning emission was similar to our findings. *Feng et al.* [2018] reported that anthropogenically-emitted CH_2Cl_2 increased from 2005 to 2016, contrary to our findings. There might be two causes. Firstly, the estimation by *Feng et al.* [2018] was for the whole China while local situations in different regions might be different. Secondly, the insignificant changes found in this study might be owing to limited sampling years. Since CH_2Cl_2, $CHCl_3$ and CH_3Cl did not decline, their emissions should be controlled through more stringent measures.

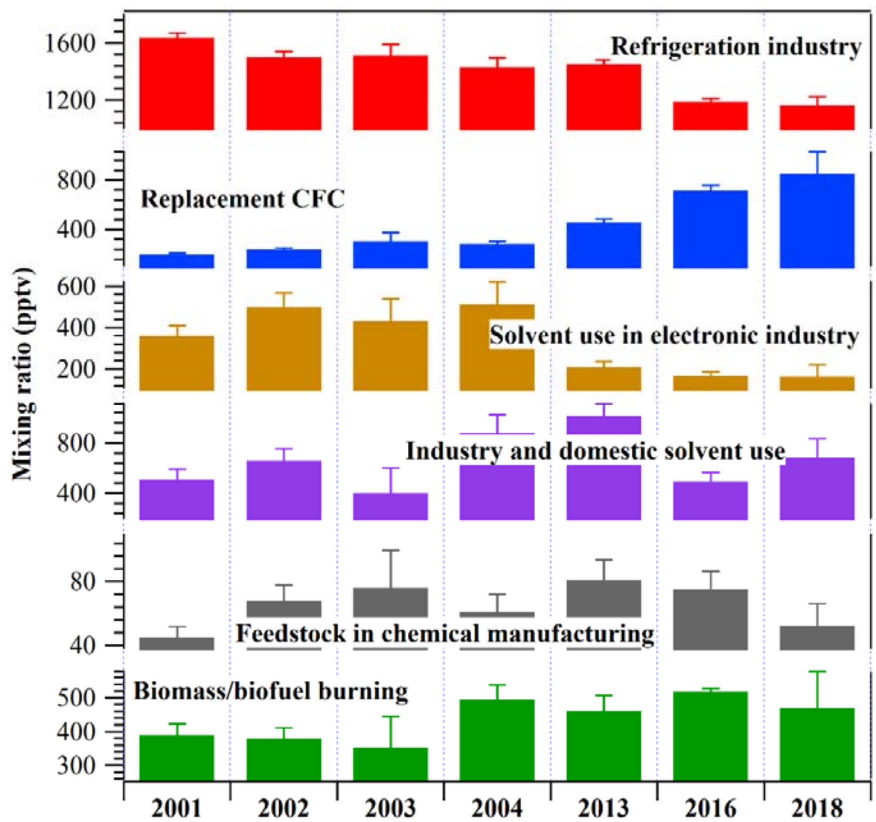

Figure 4. Source Contributions to the Total Halocarbons in the Greater PRD region (mean ± 95% confidence interval) in 2001, 2002, 2003, 2004, 2013, 2016, 2018

3.5 Halocarbon Emission Estimates in the Greater PRD region

The CO emissions used for halocarbon emission estimations in the inner PRD and HK were 7305.40 Gg in 2012 (latest available CO emission inventory) with an uncertainty of ±68% and 58.52 Gg with an uncertainty of ±29% in 2016, respectively [*Zhong et al*., 2018; *HKEPD,2018b*]. Here we assumed that total CO emission in 2016 in the Greater PRD region was 7363.92 Gg. Scatter plots of mixing ratios of halocarbons versus CO values are shown in Figure S4. The slopes were applied for the emission estimation. As shown in Table 4, the total halocarbon emission in the Greater PRD region was estimated to be 46.5±16.7 Gg. By comparison, our results were basically consistent with or lower than the estimated halocarbon emissions in 2001, 2004, 2009 and 2010 in previous studies [*Guo et al*., 2009; *Shao et al*., 2011; *Zhang et al*., 2014], except for CFC-11, CFC-114, HCFC-22, CH_3Cl and CH_2Cl_2. Specifically, our estimated emissions of CFC-11 and CFC-114 in 2016 were higher than those in 2004, 2009 and 2010, suggesting possible new sources of these two species in recent years.

Among the target halocarbons in the Greater PRD region, the highest estimated emission was from CH_2Cl_2 (21±7.8 Gg) accounting for 45% of the total emissions, implying significant contributions of solvent use and chemical manufacturing to ambient halocarbons. The estimated emission of CH_2Cl_2 was much lower than that in 2001 but higher than the emission in 2004. CH_3Cl had similar temporal variations in estimated emission to CH_2Cl_2. Thus, tighter control measures are needed to reduce these two species. The estimated CFCs emission (2.6±1.3 Gg) was much lower than those of HCFC-22 and HFC-134a (15±3.9 Gg), in line with the successful replacement of CFCs with HCFCs and HFCs in this region. Moreover, the estimated emission of HCFC-22 was higher than previous levels, in agreement with its increasing ambient levels. *Saikawa et al.* [2012] also estimated the increase in HCFC-22 emissions from Article-5 Asia during 2005-2010. Since both HCFC-22 and HFC-134a are in the restriction list and need to be phased out in the next phase, controlling their emissions would pose a challenge to this region. The emissions of other halocarbons (mainly used in solvents and chemical manufacturing) in the Greater PRD region (29±11 Gg) accounted for 62% of the total emissions, implying increased use of short-lived halocarbons. Among these short-lived species, the estimated emissions of CH_3CCl_3 and C_2Cl_4 decreased dramatically compared to previous estimations, mainly due to effective regulations. It is noteworthy that the technique used here is a very rough estimate of halocarbon emissions with some uncertainties. As the sources, lifetime and chemical properties of halocarbons and CO have some differences, the estimated halocarbon emissions would have some uncertainties using the ratio of the enhancement of halocarbon to CO. Furthermore, the CO emission inventory also has some uncertainties. Therefore, other approaches such as a better reference species for inter-species correlations [*Wu et al.*, 2014] and/or inverse model simulations should be explored in future studies [*Fang et al.*, 2015].

Table 4. Measured Halocarbons: CO Relationships and Estimated Halocarbon Emissions (in Gg) in 2016

Compounds	M ($g \cdot mol^{-1}$)	The Greater PRD region (n=218)[a]			Reference value in PRD region (Gg)			
		Ratio	Pearson correlation coefficient	Emission estimation (Gg)	2001[d]	2004[e]	2009[f]	2010[g]
CFC-11	137.36	0.05±0.02	0.18	1.7±0.9	1.0 ± 0.3	0.4±0.2	0.5±0.1	0.9
CFC-12	120.91	0.01±0.005	0.17	0.4±0.2	1.5 ± 0.4	1.6±1.0	1.2±0.3	1.6
CFC-113	187.38	0.004±0.002	0.11	0.2±0.1	0.9 ± 0.3	0.0±0.0	0.2±0.04	
CFC-114	170.92	0.006±0.001	0.48	0.3±0.05		0.0±0.0	0.1±0.01	
HCFC-22	86.47	0.54±0.13	0.41	12±3.0	2.2±1.2	3.5±2.2	2.5±0.7	10.7
HFC-134a	102.03	0.12±0.03	0.22	3.1±0.9				1.3
CH_3Cl	50.49	0.35±0.33	0.18	4.6±2.0	2.8 ± 0.5	0.6±0.4		
CH_3CCl_3	133.40	0.006±0.0008	0.41	0.2±0.03		0.4±0.2		
CH_2Cl_2	84.93	1.02±0.35	0.29	21±7.8	42.8 ± 7.2	7.0±4.6		
CCl_4	153.81	0.02±0.004	0.24	0.8±0.2	0.7 ± 0.2	1.1±0.7		
$CHCl_3$	119.37	0.03±0.02	0.34	0.9±0.6	2.4 ± 1.8	0.8±0.6		
C_2Cl_4	165.82	0.03±0.02	0.38	1.3±0.9	7.3 ± 1.5	2.3±1.5		
Sum				46.5±16.7				
CO	28.01			7363.92[b, c]				

a. The parameter n is the number of samples; the ratio is the regression slope of Δhalocarbon against ΔCO (pptv/ppbv); Pearson correlation coefficient is the parameter of determination of the ratio; b. HKEPD public data, https://www.epd.gov.hk/epd/sc_chi/environmentinhk/air/data/emission_inve_co_C.html; c. [*Zhong et al.*, 2018]; d. [*Guo et al.*, 2009]; e. [*Shao et al.*, 2011]; f. [*Zhang et al.*, 2014]; g. [*Wu et al.*, 2014].

4. Conclusions

In this study, we investigated long-term temporal variations, source changes and emissions of halocarbons in the Greater PRD region from 2001 to 2018 based on 1505 whole air samples. CH_3Cl was the most abundant halocarbon, followed by CH_2Cl_2, HCFC-22 and CFC-12. Long-term analysis indicated significantly (p<0.005) decreasing trends of CFC-11, CFC-12, CFC-113 and H-1211, and increases in HFC-134a, HCFC-22 and CFC-114 in the past 18 years in the Greater PRD region. Compared to the variation rates at the background MLO site, faster declines of CFCs (CFC-11, CFC-12 and CFC-113) in the Greater PRD region suggested effectiveness of previous/ongoing control measures under the Montreal Protocol. In addition, though mixing ratios of CCl_4, CH_3CCl_3 and C_2Cl_4 decreased significantly (p<0.005), the values of CH_2Cl_2, CH_3Cl, and CH_3I remarkably increased (p<0.05), indicating more stringent control regulations are still needed. In particular, CH_2Cl_2 showed the highest growth rate in the Greater PRD region.

Source apportionment results revealed that halocarbons in the Greater PRD were mainly used in refrigerants applications, including refrigeration industry and replacement of CFCs, in these years. Contribution of refrigeration industry showed a decline during 2001-2018, while source of replacement of CFCs increased progressively. Furthermore, solvent use in electronic industry made invariable contributions during 2001-2004, but the contribution dramatically decreased in 2013 and remained at a low level in recent years. The contributions of industrial/domestic solvent use, feedstock in chemical manufacturing and biomass/biofuel burning did not change significantly during the study period and required further control measures.

According to the ratio of halocarbon to CO and the CO emissions, the total halocarbon emissions in 2016 were estimated to be 46.5 ± 16.7 Gg for the Greater PRD. The estimated emission of CH_2Cl_2 was the largest, suggesting significant contributions of industrial and domestic solvent use to ambient halocarbons in the Greater PRD region. The findings advanced our knowledge on halocarbons in the Greater PRD region.

Acknowledgements

The authors thank the financial support by the National Key R&D Program of China via grant No. 2017YFC0212001. This study was supported by the Research Grants Council of the Hong Kong Special Administrative Region Government via grants

PolyU152052/14E, PolyU152052/16E and CRF/C5004-15E, and the Public Policy Research Funding Scheme from Policy Innovation and Co-ordination Office of the Hong Kong Special Administrative Region Government (Project Number: 2017.A6.094.17D). The data at Mauna Loa station provided by the National Oceanic and Atmospheric Administration (NOAA) is highly appreciated.

References

Barletta, B., Meinardi, S., Simpson, I. J., Rowland, F. S., Chan, C. Y., Wang, X. M., Zou, S. C., Chan, L. Y. and Blake, D. R. (2006), Ambient halocarbon mixing ratios in 45 Chinese cities, *Atmospheric Environment*, 40(40), 7706-7719.

Blake, N. J., Blake, D. R., Sive, B. C., Chen, T.-Y., Rowland, F. S., Collins Jr., J. E., Sache, G. W. and Anderson, B. E. (1996), Biomass burning emissions and vertical distribution of atmospheric methyl halides and other reduced carbon gases in the South Atlantic region, *Journal of Geophysical Research: Atmospheres*, 101, 24151-24164.

Borkar, C., Tomar, D. and Gumma S. (2010), Adsorption of Dichloromethane on Activated Carbon, *Journal of Chemical & Engineering Data*, 55(4), 1640-1644.

Carpenter, L. J., Reimann, S., Burkholder, J. B., Clerbaux, C., Hall, B. D., Hossaini, R., Laube, J. C. and Yvon-Lewis, S. A. (2014), Update on ozone-depleting substances (ODSs) and other gases of interest to the Montreal protocol, *Scientific assessment of ozone depletion*: 2014, 1-1.

Chan, C. Y., Tang, J. H., Li, Y. S. and Chan, L. Y. (2006b), Mixing ratios and sources of halocarbons in urban, semi-urban and rural sites of the Pearl River Delta, South China, *Atmospheric Environment*, 40(38), 7331-7345.

Chan, L. Y. and Chu, K. W. (2007), Halocarbons in the atmosphere of the industrial-related Pearl River Delta region of China, *Journal of Geophysical Research: Atmospheres*, *112*(D4), doi:doi:10.1029/2006JD007097.

Chan, J. Y., Tang, J. H., Li, Y. S. and Chan, L. Y. (2006a), Mixing ratios and sources of halocarbons in urban, semi-urban and rural sites of the Pearl River Delta, South China, *Atmospheric Environment*, 40(38), 7331-7345.

Chang, C. C., Lai, C. H., Wang, C. H., Liu, Y., Shao, M., Zhang, Y. and Wang, J. L. (2008), Variability of ozone depleting substances as an indication of emissions in the Pearl River Delta, China, *Atmospheric Environment*, 42(29), 6973-6981.

CFOMIA (2016), China Fluorosilicone Organic Materials Industry Association, China's fluorine chemical industry "13th five-year" development plan, http://www.sif.org.cn/.

CHP (2018), The Health Effects of Air Pollution, https://www.chp.gov.hk/en/healthtopics/content/460/3557.html.

Devotta, S., Waghmare, A. V., Sawant, N. N. and Domkundwar, B. M. (2001), Alternatives to HCFC-22 for air conditioners, *Applied Thermal Engineering*, 21(6), 703-715.

ESRL (2018), https://www.esrl.noaa.gov/gmd/dv/data/index.php?category=Halocompounds.

Fang, X. K., Wu, J., Su, S. S., Han, J. R., Wu, Y. S., Shi, Y. H., Wan, D., Sun, X. Z., Zhang, J. B. and Hu, J. X. (2012), Estimates of major anthropogenic halocarbon emissions from China based on interspecies correlations, *Atmospheric Environment*, 62, 26-33.

Fang, X. K., Stohl, A., Yokouchi, Y., Kim, J., Li, S., Saito, T., Park, S. and Hu, J. (2015), Multiannual top-down estimate of HFC-23 emissions in East Asia, *Environmental Science & Technology*, 49(7), 4345-4353.

Fang X. K., Park, S., Saito, T., Tunnicliffe, R., Ganesan, A. L., Rigby, M., Li, S. L., Yokouchi, Y., Fraser, P. J., Harth, C. M., Krummel, P. B., Mühle, J., O'Doherty, S., Salameh, P. K., Simmonds, P. G., Weiss, R. F., Young, D., Lunt, M. F., Manning, A. J., Gressent, A. and Prinn, R. G. (2019), Rapid increase in ozone-depleting chloroform emissions from China, *Nature Geoscience*, 12, 89-93.

Fang, X., Velders, G. J. M., Ravishankara, A. R., Molina, M. J., Hu, J. and Prinn, R. G. (2016), Hydrofluorocarbon (HFC) Emissions in China: An Inventory for 2005–2013 and Projections to 2050, *Environmental Science & Technology*, 50(4), 2027-2034.

Feng, Y., Bie, P., Wang, Z., Wang, L. and Zhang, J. (2018), Bottom-up anthropogenic dichloromethane emission estimates from China for the period 2005–2016 and predictions of future emissions, *Atmospheric Environment*, 186, 241-247.

Fiehn, A., Quack, B., Hepach, H., Fuhlbrügge, S., Tegtmeier, S., Toohey, M., Atlas, E. and Krüger, K. (2017), Delivery of halogenated very short-lived substances from the West Indian Ocean to the stratosphere during Asian summer monsoon, *Atmospheric Chemistry and Physics*, 17, 6723-6741.

Fortems-Cheiney, A., Chevallier, F., Saunois, M., Pison, I., Bousquet, P., Cressot, C., Wang, H. J., Yokouchi, Y. and Artuso, F. (2013), HCFC-22 emissions at global and regional scales between 1995 and2010: Trends and variability, *Journal of Geophysical Research: Atmospheres*, 118(13), 7379-7388.

Fraser, P. J., Oram, D. E., Reeves, C. E., Penkett, S. A. and McCulloch, A. (1999), Southern Hemispheric halon trends (1978–1998) and global halon emissions, *Journal of Geophysical Research: Atmospheres*, 104(D13), 15985-15999.

Fuhlbrügge, S., Quack, B., Tegtmeier, S., Atlas, E., Hepach, H., Shi, Q., Raimund, S. and Krüger, K. (2016), The contribution of oceanic halocarbons to marine and free troposphere air over the tropical West Pacific, *Atmospheric Chemistry and Physics*, 16(12), 7569-7585.

Gentner, D. R., Miller, A. M. and Goldstein, A. H. (2010), Seasonal Variability in Anthropogenic Halocarbon Emissions, *Environmental Science & Technology*, 44(14), 5377-5382.

Godish, T. (2003), Air quality (Fourth edition), Lewis Books, Boca Raton, Florida.

Grubb, M., Vrolijk, C. and Brack, D. (1999), The Kyoto Protocol. A guide and assessment, *Molecular Ecology*, 13(8), 2121-2133.

Guo, H., Ding, A.J., Wang, T., Simpson, I.J., Blake, D.R., Barletta, B., Meinardi, S., Rowland, F. S., Saunders, S.M., Fu, T.M., Hung, W.T. and Li, Y.S. (2009), Source origins, modeled profiles, and apportionments of halogenated hydrocarbons in the greater Pearl River Delta region, southern China, *Journal of Geophysical Research: Atmospheres*, 114, 19, D11302.

Harrison, J. J., Boone, C. D. and Bernath, P. F. (2017), New and improved infra-red absorption cross sections and ACE-FTS retrievals of carbon tetrachloride (CCl_4), *Journal of Quantitative Spectroscopy and Radiative Transfer*, 186, 139-149.

HKEPD, (2018a), https://www.epd.gov.hk/epd/english/environmentinhk/air/data/phase_out.html.

HKEPD, (2018b), https://www.epd.gov.hk/epd/sc_chi/environmentinhk/air/data/emission_inve_co_C.html.

Hundy, G.F., Trott, A.R. and Welch, T.C. (2016), Refrigeration, Air Conditioning and Heat Pumps. 5th Edition, Elsevier Ltd, London.

Hurst D. F., Romashkin, P. A., Elkins, J. W., Oberländer, E. A., Elansky, N. F., Belikov, I. B., Granberg, I. G., Golitsyn, G. S., Grisenko, A. M., Brenninkmeijer, C. A. M. and Crutzen, P. J. (2004), Emissions of ozone‐depleting substances in Russia during 2001, *J. Geophys. Res.*, 109, D14303.

Hurst, D. F., Lin, J. C., Romashkin, P. A., Daube, B. C., Gerbig, C., Matross, D. M., Wofsy, S. C., Hall, B. D. and Elkins, J. W. (2006), Continuing global significance of emissions of Montreal Protocol-restricted halocarbons in the United States and Canada, *Journal of Geophysical Research: Atmospheres*, 111(D15), 15.

Kock, H. H., Bieber, E., Ebinghaus, R., Spain, T. G., and Thees, B. (2005), Comparison of long-term trends and seasonal variations of atmospheric mercury concentrations at the two European coastal monitoring stations Mace Head, Ireland, and Zingst, Germany, *Atmospheric Environment*, 39(39), 7549-7556.

Laube, J. C., Mohd Hanif, N., Martinerie, P., Gallacher, E., Fraser, P.J., Langenfelds, R., Brenninkmeijer, C.A.M., Schwander, J., Witrant, E., Wang, J.-L., Ou-Yang, C.F., Gooch, L.J., Reeves, C.E., Sturges, W.T. and Oram, D.E. (2016), Tropospheric observations of CFC-114 and CFC-114a with a focus on long-term trends and emissions, *Atmospheric Chemistry & Physics*, 16(23), 15347-15358.

Lee, S. C., Chiu, M. Y., Ho, K. F., Zou, S. C. and Wang, X. (2002), Volatile organic compounds (VOCs) in urban atmosphere of Hong Kong, *Chemosphere*, 48(3), 375-382.

Leedham Elvidge, E. C., Oram, D. E., Laube, J. C., Baker, A. K., Montzka, S. A., Humphrey, S., O'Sullivan, D. A. and Brenninkmeijer, C. A. M. (2015), Increasing concentrations of dichloromethane, CH_2Cl_2, inferred from CARIBIC air samples collected 1998–2012, *Atmospheric Chemistry & Physics*, 15(4), 1939-1958.

Lennartz, S. T., Krysztofiak, G., Marandino, C. A., Sinnhuber, B.-M., Tegtmeier, S., Ziska1, F., Hossaini, R., Krüger, K., Montzka, S. A., Atlas, E., Oram, D. E., Keber, T., Bönisch, H. and Quack, B. (2015), Modelling marine emissions and atmospheric distributions of halocarbons and dimethyl sulfide: the influence of prescribed water concentration vs. prescribed emissions, *Atmospheric Chemistry & Physics*, 15(20), 11753-11772.

Li, S., Park, M.-K., Jo, C. O. and Park, S. (2017), Emission estimates of methyl chloride from industrial sources in China based on high frequency atmospheric observations, *Journal of Atmospheric Chemistry*, 74(2), 227-243.

Ling, Z. H., Guo, H., Lam, S. H. M., Saunders, S. M. and Wang, T. (2014), Atmospheric photochemical reactivity and ozone production at two sites in Hong Kong: Application of a Master Chemical Mechanism–photochemical box model, *Journal of Geophysical Research: Atmospheres*, 119(17), 10567-10582.

Lunt, M. F., Park, S., Li, S., Henne, S., Manning, A. J., Ganesan, A. L., Simpson, I. J., Blake, D. R., Liang, Q., O'Doherty, S., Harth, C. M., Mühle, J., Salameh, P. K., Weiss, R. F., Krummel, P. B., Fraser, P. J., Prinn, R. G., Reimann, S. and Rigby, M. (2018), Continued emissions of the ozone-depleting substance carbon tetrachloride from Eastern Asia, *Geophysical Research Letters*, 45(20), 11324-11430.

Maione, M., Giostra, U., Arduini, J., Furlani, F., Bonasoni, P., Cristofanclli, P., Laj, P. and Vuillermoz, E. (2011), Three-year observations of halocarbons at the Nepal Climate Observatory at Pyramid (NCO-P, 5079 m a.s.l.) on the Himalayan range, *Atmospheric Chemistry & Physics*, 11(7), 3431-3441.

Montzka, S. A., Dutton, G. S., Yu, P., Ray, E., Portmann, R. W., Daniel, J. S., Lambert, K., Hall, B. D., Mondeel, D., Siso, C., Nance, J. D., Rigby, M., Manning, A. J., Hu, L., Moore, F., Miller, B. R. and Elkins, J. W. (2018), An unexpected and persistent increase in global emissions of ozone-depleting CFC-11, *Nature*, 557, 413-417.

Oram, D. E., Ashfold, M. J., Laube, J. C., Gooch, L. J., Humphrey, S., Sturges, W. T., Leedham-Elvidge, E., Forster, G. L., Harris, N. R. P., Mead, M. I., Samah, A. A., Phang, S. M., Ou-Yang, C. F., Lin, N. H., Wang, J. L., Baker, A. K., Brenninkmeijer, C. A. M. and Sherry, D. (2017), A growing threat to the ozone layer from short-lived anthropogenic chlorocarbons, *Atmospheric Chemistry & Physics,* 17(19), 11929-11941.

Ou-Yang, C. F., Chang, C. C., Chen, S. P., Chew, C., Lee, B. R., Chang, C. Y., Montzka, S. A., Dutton, G. S., Butler, J. H. and Elkins, J. W. (2015), Changes in the levels and variability of halocarbons and the compliance with the Montreal Protocol from an urban view, *Chemosphere*, 138, 438-446.

Paatero, P. (1997), Least squares formulation of robust non-negative factor analysis, *Chemometrics & Intelligent Laboratory Systems*, 37(1), 23-35.

Palmer, P. I., Jacob, D. J., Mickley, L. J., Blake, D. R., Sachse, G. W., Fuelberg, H. E. and Kiley, C. M. (2003), Eastern Asian emissions of anthropogenic halocarbons deduced from aircraft concentration data, *Journal of Geophysical Research: Atmospheres*, 108(D24), 4753.

Prinn, R. G., Cunnold, D. M., Rasmussen, R., Simmonds, P. G., Alyea, F. N., Crawford, A., Fraser, P. J. and Rosen, R. (1987), Atmospheric trends in methylchloroform and the global average for the hydroxyl radical, *Science*, 238, 945-950.

Qin, D. (2007), Decline in the concentrations of chlorofluorocarbons (CFC-11, CFC-12 and CFC-113) in an urban area of Beijing, China, *Atmospheric Environment*, 41(38), 8424-8430.

Rasmussen, R. A., Khalil, M. A. K., Gunawardena, R. and Hoyt, S. D. (1982), Atmospheric Methyl Iodide (CH_3I), *Journal of Geophysical Research: Oceans*, 87(C4), 3086-3090.

Rigby, M., Park, S., Saito, T., Western, L. M., Redington, A. L., Fang, X., Henne, S., Manning, A. J., Prinn, R. G., Dutton, G. S., Fraser, P. J., Ganesan, A. L., Hall, B. D., Harth, C. M., Kim, J., Kim, K. –R., Krummel, P. B., Lee, T., Li, S., Liang, Q., Lunt, M. F., Montzka, S. A., Mühle, J., O'Doherty, S., Park, M. –K., Reimann, S., Salameh, P. K., Simmonds, P., Tunnicliffe, R. L., Weiss, R. F., Yokouchi, Y. and Young, D. (2019), Increase in CFC-11 emissions from eastern China based on atmospheric observations., *Nature*, 569(7757), 546.

Rossberg, M., Lendle, W., Pfleiderer, G., Tögel, A., Torkelson, T. R. and Beutel, K. K. (2011), *Chloromethanes*, Wiley-VCH Verlag GmbH & Co. KGaA.

Saikawa, E., Rigby, M., Prinn, R. G., Montzka, S. A., Miller, B. R., Kuijpers, L. J., Fraser, P. J. B., Vollmer, M. K., Saito, T., Yokouchi, Y., Harth, C. M., Mühle, J., Weiss, R. F., Salameh, P. K., Kim, J., Li, S., Park, S., Kim, K. –R., Young, S., O'Doherty, S., Simmonds, P. G., McCulloch, A., Krummel, P. B., Steele, L. P., Lunder, C., Hermansen, O., Maione, M., Arduini, J., Yao, B., Zhou, L. X., Wang, H. J., Elkins, J. W. and Hall, B. (2012), Global and regional emission estimates for HCFC-22, *Atmospheric Chemistry and Physics*, 12(21), 10033-10050.

Scheeren, H. A., Lelieveld, J., De Gouw, J. A., Van der Veen, C. and Fischer, H. (2002), Methyl chloride and other chlorocarbons in polluted air during INDOEX, *Journal of Geophysical Research: Atmospheres*, 107(D19), INX2-14.

Seinfeld, J.H. and Pandis, S.N. (2016), Atmospheric Chemistry and Physics: From Air Pollution to Climate Change. John Wiley & Sons, Hoboken.

Shao, M., Huang, D., Gu, D., Lu, S., Chang, C. and Wang, J. (2011), Estimate of anthropogenic halocarbon emission based on measured ratio relative to CO in the Pearl River Delta region, China, *Atmospheric Chemistry & Physics*, 11(10), 5011-5025.

Sikdar, S. K. (2001), Process design tools for the environment, *Crc Press*, *99*(2), 223-223.

Simmonds, P. G., Cunnold, D. M., Weiss, R. F., Prinn, R. G., Fraser, P. J., McCulloch, A., Alyea, F. N. and O'Doherty, S. (1998), Global trends and emission estimates of CCl4 from in situ background observations from July 1978 to June 1996, *Journal of Geophysical Research: Atmospheres*, 103(D13), 16017-16027.

Simmonds, P. G., Manning, A. J., Cunnold, D. M., McCulloch, A., O'Doherty, S., Derwent, R. G., Krummel, P. B., Fraser, P. J., Dunse, B., Porter, L. W., Wang, R. H. J., Greally, B. R., Miller, B. R., Salameh, P., Weiss, R. F. and Prinn, R. G. (2006), Global trends, seasonal cycles, and European emissions of dichloromethane, trichloroethene, and tetrachloroethene from the AGAGE observations at Mace Head, Ireland, and Cape Grim, Tasmania, *Journal of Geophysical Research: Atmospheres*, 111(D18), D18304.

Simmonds, P. G., Rigby, M., Mcculloch, A., O'Doherty, S., Young, D., Mühle, J., Krummel, P. B., Steele, P., Fraser, P. J. and Manning, A. J. (2017), Changing trends and emissions of hydrochlorofluorocarbons (HCFCs) and their hydrofluorocarbon (HFCs) replacements, *Atmospheric Chemistry & Physics*, 17(7), 4641-4655.

Simpson, I. J., Meinardi, S., Blake, N. J., Rowland, F. S. and Blake, D. R. (2004), Long-term decrease in the global atmospheric burden of tetrachloroethene (C_2Cl_4), *Geophysical Research Letters*, 31(8), L08108.

Stratosphere-troposphere Processes And their Role in Climate (SPARC) (2017), SPARC Report on the Mystery of Carbon Tetrachloride, Q. Liang, P. A. Newman, and S. Reimann (Eds.), *SPARC Report No. 7*, WCRP-13/2016.

Su, S. S., Fang, X. K., Li, L., Wu, J., Zhang, J. B., Xu, W. G. and Hu, J. X. (2015), HFC-134a emissions from mobile air conditioning in China from 1995 to 2030, *Atmospheric Environment*, 102, 122-129.

Thompson, A. E., Anderson, R. S., Rudolph, J. and Huang, L. (2002), Stable carbon isotope signatures of background tropospheric chloromethane and CFC113, *Biogeochemistry*, 60(2), 191-211.

Varner, R. K., Crill, P. M., Talbot, R. W. and Shorter, J. H. (1999), An estimate of the uptake of atmospheric methyl bromide by agricultural soils, *Geophysical research letters*, 26(6), 727-730.

Velders, G. J. M., Fahey, D. W., Daniel, J. S., Andersen, S. O. and McFarland, M. (2015), Future atmospheric abundances and climate forcings from scenarios of global and regional hydrofluorocarbon (HFC) emissions, *Atmospheric Environment*, 123, 200-209.

Vollmer, M. K., Zhou, L. X., Greally, B. R., Henne, S., Yao, B., Reimann, S., Stordal, F., Cunnold, D. M., Zhang, X. C., Maione, M., Zhang, F, Huang, J. and Simmonds, P. G. (2009), Emissions of ozone-depleting halocarbons from China. *Geophysical research letters*, 36 (15), L15823.

Vollmer, M. K., Young, D., Trudinger, C. M., Mühle, J., Henne, S., Rigby, M., Park, S., Li, S., Guillevic, M., Mitrevski, B., Harth, C. M., Miller, B. R., Reimann, S., Yao, B., Steele, L. P., Wyss, S. A., Lunder, C. R., Arduini, J., McCulloch, A., Wu, S. H., Rhee, T. S., Wang, R. H. J., Salameh, P. K., Hermansen, O., Hill, M., Langenfelds, R. L., Ivy, D., O'Doherty, S., Krummel, P. B., Maione, M., Etheridge, D. M., Zhou, L. X., Fraser, P. J., Prinn, R. G., Weiss, R. F. and Simmonds, P. G. (2018), Atmospheric histories and emissions of chlorofluorocarbons CFC-13 ($CClF_3$), ΣCFC-114 ($C_2Cl_2F_4$), and CFC-115 (C_2ClF_5), *Atmospheric Chemistry & Physics*, 18(2), 979-1002.

Wang, C., Shao, M., Huang, D. K., Lu, S. H., Zeng, L. M., Hu, M. and Zhang, Q. (2014), Estimating halocarbon emissions using measured ratio relative to tracers in China, *Atmospheric Environment*, 89, 816-826.

Wang, T., Guo, H., Blake, D. R., Kwok, Y. H., Simpson, I. J. and Li, Y. S. (2005), Measurements of Trace Gases in the Inflow of South China Sea Background Air and Outflow of Regional Pollution at Tai O, Southern China, *Journal of Atmospheric Chemistry*, 52(3), 295.

Wang, W., Liu, X., Zhao, L., Guo, D., Tian, X., & Adams, F. (2006), Effectiveness of leaded petrol phase-out in Tianjin, China based on the aerosol lead concentration and isotope abundance ratio, *Science of the Total Environment*, 364 (1-3), 175-187.

Wang, Y., Guo, H., Zou, S. C., Lyu, X. P., Ling, Z. H., Cheng, H. R. and Zeren Y. Z. (2018), Surface O_3 photochemistry over the South China Sea: Application of a near-explicit chemical mechanism box model, *Environmental Pollution*, 234, 155-166.

WMO/UNEP (2018), Scientific Assessment of Ozone Depletion: 2018, Global Ozone Research and Monitoring Project. Report no. 58.88. https://www.esrl.noaa.gov/csd/assessments/ozone/2018/.

Wu, J., Fang, X. K., Xu, W. Y., Wan, D., Shi, Y. H., Su, S. S., Hu, J. X. and Zhang, J. B. (2013), Chlorofluorocarbons, hydrochlorofluorocarbons, and hydrofluorocarbons in the atmosphere of four Chinese cities, *Atmospheric Environment*, 75, 83-91.

Wu, J., Fang, X.K., Martin, J. W., Zhai, Z.H., Su, S.S., Hu, X., Han, J.R., Lu, S. H., Wang, C., Zhang, J. B. and Hu, J. X. (2014), Estimated emissions of chlorofluorocarbons, hydrochlorofluorocarbons, and hydrofluorocarbons based on an interspecies correlation method in the Pearl River Delta region, China, *Science of the Total Environment*, 470–471, 829–834.

Xue, L. K., Wang, T., Simpson, I. J., Ding, A. J., Gao, J., Blake, D. R., Wang, X. Z., Wang, W. X., Lei, H. C. and Jin, D. Z. (2011), Vertical distributions of non-methane hydrocarbons and halocarbons in the lower troposphere over northeast China, *Atmospheric environment*, 45(36), 6501-6509.

Yin, L., Du, P., Zhang, M., Xu, T. and Song, Y. (2019), Estimation of emissions from biomass burning in China (2003–2017) based on MODIS fire radiative energy data, *Biogeosciences*, 16(7), 1629-1640.

Yin, Y., Li, Y., Tai, C., Cai, Y. and Jiang, G. (2014), Fumigant methyl iodide can methylate inorganic mercury species in natural waters, *Nature Communications*, 5, 4633.

Yokouchi, Y., Noijiri, Y., Barrie, L. A., Toom-Sauntry, D., Machida, T., Inuzuka, Y., Akimoto, H., Li, H. –J., Fujinuma, Y., and Aoki, S. (2000), A strong source of methyl chloride to the atmosphere from tropical coastal land, *Nature*, 403(6767), 295-298.

Yokouchi, Y., Toom-Sauntry, D., Yazawa, K., Inagaki, T. and Tamaru, T. (2002), Recent decline of methyl bromide in the troposphere, *Atmospheric Environment*, 36(32), 4985-4989.

Yokouchi, Y., Nojiri, Y., Toom-Sauntry, D., Fraser, P., Inuzuka, Y., Tanimoto, H., Nara, H., Murakami, R. and Mukai, H. (2012), Long-term variation of atmospheric methyl iodide and its link to global environmental change, *Geophysical research letters*, 39(23), L23805, doi: 10.1029/2012GL053695.

Yvon-Lewis, S. A., Saltzman, E. S. and Montzka, S. A. (2009), Recent trends in atmospheric methyl bromide: analysis of post-Montreal Protocol variability, *Atmospheric Chemistry and Physics*, *9*(16), 5963-5974.

Zhang, F., Zhou, L.X., Yao, B., Vollmer, M.K., Greally, B.R., Simmonds, P.G., Frode Stordal, S.R., Maione, M., Xu, L. and Zhang, X. C. (2010a), Analysis of 3-year observations of CFC-11, CFC-12 and CFC-113 from a semi-rural site in China, *Atmospheric Environment*, 44(35), 4454-4462.

Zhang, F., Zhou, L. X., Yao, B., Vollmer, M. K., Greally, B. R., Simmonds, P. G., Reimann, S., Stordal, F., Maione, M., Xu, L., and Zhang, X. C, (2010c), Analysis of 3-year observations of CFC-11, CFC-12 and CFC-113 from a semi-rural site in China, *Atmospheric Environment*, 44(35), 4454-4462.

Zhang, Y. H., Hu, M., Zhong, L. J., Wiedensohler, A., Liu, S. C., Andreae, M. O., Wang, W., and Fan, S. J. (2008), Regional Integrated Experiments on Air Quality over Pearl River Delta 2004 (PRIDE-PRD2004): Overview, *Atmospheric Environment*, 42(25), 6157-6173.

Zhang Y. L., Guo H., Wang X. M., Simpson I. J., Barletta, B., Blake, D. R., Meinardi, S., Rowland, F. S., Cheng, H. R., Saunders, S. M. and Lam, S. H. M. (2010b), Emission patterns and spatiotemporal variations of halocarbons in the Pearl River Delta region, southern China, *Journal of Geophysical Research: Atmospheres*, 115, 16.

Zhang Y. L., Wang, X. M., Simpson, I. J., Barletta, B., Blake, D. R., Meinardi, S., Louie, P. K. K., Zhao, X. Y., Shao, M., Zhong, L. J., Wang, B. G. and Wu, D. (2014), Ambient CFCs and HCFC-22 observed concurrently at 84 sites in the Pearl River Delta region during the 2008-2009 grid studies, *Journal of Geophysical Research: Atmospheres*, 119(12), 7699-7717.

Zhong, Z. M., Zheng, J. Y., Zhu, M. N., Huang, Z. J., Zhang, Z. W., Jia, G. L., Wang, X. L., Bian, Y. L., Wang Y. L. and Li, N. (2018). Recent developments of anthropogenic air pollutant emission inventories in Guangdong province, China. *Science of the Total Environment*, 627, 1080-1092.